J of Nuclear Medicine Technology, first published online September 4, 2020 as doi:10.2967/jnmt.120.249680

Evaluation of 111In-Pentetreotide single photon emission computed tomography imaging correction method for gastroenteropancreatic neuroendocrine tumors

Takao Kanzaki[1,2*], Yasuyuki Takahashi[2], Tetsuya Higuchi[3], Xieyi Zhang[4], Nao Mogi[1], Takayuki Suto[1], Yoshito Tsushima[3]

1. Department of Radiology, Gunma University Hospital
   3-39-15 Showa, Maebashi, Gunma 371-8511 Japan
2. Department of Nuclear Medicine Technology, Hirosaki University Graduate School of Health Sciences
   66-1 Hon-cho, Hirosaki, Aomori 036-8564 Japan
3. Department of Diagnostic Radiology and Nuclear Medicine, Gunma University Graduate School of Medicine
   3-39-22 Showa, Maebashi, Gunma 371-8511 Japan
4. Laboratory of Biopharmaceutics, Department of Pharmacology, Faculty of Pharmacy, Takasaki University of Health and Welfare
   60 Nakaorui-machi, Takasaki, Gunma 370-0033, Japan

Corresponding author:

Takao Kanzaki, RT, BS

Email: tkanzaki@gunma-u.ac.jp

Phone: +81-27-220-8644, Fax: +81-27-220-8644

Yasuyuki Takahashi

Email: ytaka3@hirosaki-u.ac.jp

Tetsuya Higuchi

Email: tetsuyah92md@gmail.com

Xieyi Zhang

Email: x-zhang@takasaki-u.ac.jp

Nao Mogi

Email: mogi-nao@gunma-u.ac.jp

Takayuki Suto

Email: ts1031bm@gunma-u.ac.jp

Yoshito Tsushima

Email: yoshitotsushima@gunma-u.ac.jp

Short title:

Evaluation of ^{111}In-Pentetreotide SPECT imaging correction for GEP-NET

Type of article:

Original article

Source of funding:

None

Abstract

[Purpose] The number of patients with the extremely rare disease GEP-NET (gastroenteropancreatic neuroendocrine tumor) has increased rapidly in recent years. In-111-pentetreotide single photon emission computed tomography (^{111}In-pentetreotide SPECT) in somatostatin receptor scintigraphy (SRS) has been used for the assessment of GEP-NET patients. To diagnose GEP-NET, appropriate selection of the image correction parameters is of critical importance. Correction methods may improve the ^{111}In-pentetreotide SPECT image quality, but there is currently no standard technique. The purpose of this study was to determine the optimal correction parameter settings for ^{111}In-pentetreotide SPECT imaging.

[Materials and methods] A phantom study produced scan images with a tumor-to-background ratio as high as 16:1. Triple energy window was used for scatter correction (SC), and computed tomography-based attenuation correction was used for attenuation correction (AC). Correlation analysis was performed in four groups: no correction (NC), SC, AC, and combined SC with AC corrections (CC). ^{111}In-pentetreotide SPECT results of twenty patients (13 men and 7 women; age range, 37-81 years) randomly selected patients with confirmed GEP-NET were analyzed,

using data collected four hours after injection of 111 MBq ^{111}In-pentetreotide. Emission data were reconstructed using ordered subset expectation maximization (OSEM) reconstruction, with different settings. Different combinations of the correction parameters were used to analyze the contrast to noise ratios (CNR) obtained with the phantom. In the clinical study, 20 GEP-NET patients evaluated the GEP-NET lesion CNR by four different image correction methods obtained from ^{111}In-pentetreotide SPECT images: 1) NC, 2) SC, 3) AC, and 4) CC. NC was employed as a reference method.

[Results] The phantom study revealed that the optimal energy window in the photopeak for SRS was 171 keV ± 10% and 245 keV ± 7.5%, and the optimal OSEM reconstruction conditions were 8 subsets and 6 iterations. Among the OSEM collection conditions, CC produced a significantly higher CNR than NC or SC (p<0.05). In the clinical study, CC was found to increase the CNR (p<0.05).

[Conclusion] CC improves the correction in ^{111}In-pentetreotide SPECT studies, compared with NC, providing better contrast and sharper outlines of lesions and organs.

Keywords: *Somatostatin receptor scintigraphy, ^{111}In-pentetreotide, NET*

Purpose

Neuroendocrine tumors (NETs) from neuroendocrine cells are rare, with a reported annual age-adjusted incidence of about 3-5/100,000 (*1*-*2*). Most of these tumors are derived from the gastroenteropancreatic system. However, in recent years, according to an epidemiological survey conducted in Japan, the number of patients with NETs has increased rapidly (*3*). This may be in part due to improvements in imaging and biochemical methods of detection. As advanced clinical study results for NETs became recognized, a WHO classification for gastroenteropancreatic neuroendocrine tumor (GEP-NETs) has been introduced with a grading system based on the mitotic index and Ki-67 proliferation index (*4*). NETs symptoms for diagnosis can be caused by hormonal excess, local tumor growth, metastatic spread (*5*), and high expressions of several receptors (*6*).

Recent clinical studies have indicated that In-111-pentetreotide single photon emission computed tomography (^{111}In-pentetreotide SPECT) in somatostatin receptor scintigraphy (SRS) is effective for the diagnosis and staging of GEP-NETs (*7*). In contrast, due to the small lesion size, various anatomical locations and low metabolic rate, computed tomography (CT), ultrasound, and

magnetic resonance imaging (MRI) are often insufficient for GEP-NETs diagnosis (*8*). Therefore, functional imaging with ^{111}In-pentetreotide SPECT has an important role in evaluating patients with GEP-NETs. Furthermore, multivariate analysis of GEP-NETs has revealed significant differences in age, size, depth of invasion, lymph node involvement, distant metastasis, and location. Ito *et al*. (2010) reported distant metastases in 21% of patients with non-functioning tumor-pancreatic endocrine tumors, occurring more frequently as tumor size increased (>2 cm). Lymph node metastases from gastrointestinal neuroendocrine tumors also occurred more frequently as tumor size increased (>1 cm) (*9*).

Optimization of SPECT image reconstruction for the detection of small lesions is crucial to the interpretation of ^{111}In-pentetreotide SPECT images of GEP-NETs. The ordered subset expectation maximization (OSEM) algorithm (subsets number and iteration number for a defined number of subsets) (*10*) has become the most important iterative reconstruction technique in SPECT studies. There is no standard technique of the differential correction method optimized for ^{111}In-pentetreotide SPECT imaging of GEP-NETs.

The purpose of this study was to determine the optimal correction

parameters settings for ^{111}In-pentetreotide SPECT images of GEP-NETs.

Materials and methods

Phantom study

The phantom was initially filled to simulate the quantitative outcome measures of tumor density obtained from the SPECT systems. All SPECT images were reconstructed with the use of iterative techniques including OSEM. For the first phantom study, energy window width (EWW) and OSEM reconstruction conditions were used. We used a SPECT QA Phantom (JS-10, Kyoto Kagaku Co., Ltd, Kyoto, Japan) containing five hot volumes. The phantom was initially filled at a ratio of 16:1, and background activity was simulated with uniform ^{111}In solutions of 352 kBq/ml and 22 kBq/ml. The diameters of the hot volumes were set at 7, 10, 15, 20, 30 mm. We examined whether determining the optimum EWW from the typical window locations (set at about 171 and 245 keV) was necessary. We compared results from a conventional photopeak , 15 and 20% window using four different sets of EWW parameters. In addition, the scheme of optimization of the SPECT images with use of the OSEM technique included six different sets of

reconstruction parameters. The analysis used the number of subsets (s = 8) and the variable number of iterations (i = 3 to 8).

For the second phantom study, an anthropomorphic abdominal phantom (LKS; Liver/Kidney, Kyoto Kagaku Co., Ltd, Kyoto, Japan) was used for ^{111}In-pentetreotide SPECT imaging. The tumor- Liver- background concentration ratio was 16:4:1, and background activity was simulated with uniform ^{111}In-pentetreotide solutions of 352, 88 and 22 kBq/ml (Octreoscan, FUJIFILM Toyama Chemical Co., Ltd., Tokyo, Japan). Because the SPECT QA Phantom study showed a 15-mm hot signal, we made a phantom to simulate the tumors using rods of diameter 15 mm. Based on the comparison of four correction techniques, the triple energy window was used for scatter correction (SC), while CT-based attenuation correction was used for AC. Correlation analysis was performed using four groups: no correction (NC), SC, AC, and CC (combined correction).

Clinical study

Twenty patients (13 men and 7 women; age range, 37-81 years) with suspected GEP-NET who underwent ^{111}In-pentetreotide SPECT abdomen imaging

during the period from April 2017 to April 2019 were blindly selected and enrolled in this retrospective study. Final diagnoses (20 GEP-NET) were confirmed by an endocrine physician as shown in **Table 1**. Patients were administered 111 MBq of ^{111}In-pentetreotide, and images were acquired four hours after injection. Patients did not undergo any preparation before scanning.

The study protocol was approved by the Ethics Committee of Gunma University (No. HS 2019-067).

SPECT acquisition conditions

An E-CAM (Canon Medical Systems, Otawara, Tochigi, Japan) dual-detector gamma camera system equipped with a medium- energy low-penetration collimator was used for both the phantom and clinical studies. Patients were scanned at 10-degree intervals over 360 degrees (36 s/step, 11 min in total) in a supine position using step-and-shoot and a 128 × 128 matrix. The reconstructed pixel size was 4.8 mm× 4.8 mm, zoom 1.0. The energy for ^{111}In was set at 171 keV ± 10% (20%) and 245 keV ± 7.5% (15%). With regards to energy resolution was 10.4%. The scattered radiation estimate window was set on both sides of the

photon peak window at 7% of the window width. Emission data were reconstructed by using a GMS-7700R workstation (Canon Medical Systems, Otawara, Tochigi, Japan). Reconstruction was based on the OSEM algorithm (*10*). A Butterworth filter (photopeak image: order 8, cutoff frequency of 0.50 cycles/cm, Compton scatter image: order 8, cutoff frequency of 0.4 cycles/cm for scatter correction) was used as a pre-filter.

Image processing

SC was set using triple energy windows (*11*) in which the main window was at the peak of 171 keV ± 10% and 245 keV ± 7.5%, and two additional windows for scatter correction were at 171, 245 keV ± 7%. The OSEM CTAC method was used for AC with the boundary fixed in the abdomen. The attenuation coefficient was μ= 0.135 cm^{-1}. An automatic registration tool (ART; Canon Medical Systems, Otawara, Tochigi, Japan) was used with the 320-detector CT scanner (Aquilion ONE; Canon Medical Systems, Otawara, Tochigi, Japan) data for attenuation correction of the emission images (*12*). This software tool uses two methods for automatic registration of 3D images acquired from different scanners. All CT data sets for

ART were acquired within two months from the day on which SRS was conducted. We applied OSEM with eight subsets and six iterations in the clinical study. The data were reconstructed into four groups to compare the effects of AC and SC: 1) NC, 2) SC, 3) AC, and 4) CC. In the clinical study, NC was taken as a reference, as is common in clinical practice.

Contrast-to-noise ratio of the SPECT values analysis

All SPECT data were imported into software (Daemon Research Image Processor [DRIP], FUJIFILM Toyama Chemical Co., Ltd., Tokyo, Japan). Using the SPECT QA Phantom data, we determined the optimal parameters of EWW based on the image reconstruction method and iterations in the reconstruction. Figure 1 shows an example region of interest (ROI). We evaluated the contrast-to-noise ratio (CNR) of the SPECT values in circular ROI (R1 - R5) corresponding to each rod diameter; 7, 10, 15, 20, and 30 mm in **Fig. 1**. The ROI positioning was based on the CNR method developed by Sreedhar K, *et al.* (*13*). The CNR for each sphere in the phantom was calculated as

$$\mathrm{CNR} = \left|\frac{\mathrm{C} - \mathrm{C}_B}{\sigma_{BG}}\right|$$

where *C* is the average number of counts in the sphere of interest, C_B is the average number of counts in the background (BG) ROI, and σ_{BG} is the standard deviation in the background ROI. Using LKS Phantom data, we determined the optimal imaging correction method parameters. We evaluated the CNR of the SPECT values in circular ROI (R1 – R3; Liver, pancreas and spleen) to produce a phantom simulating a tumor with a rod of diameter 15 mm, as in **Figure 1**. Similarly, In clinical study, ROI were selected in the SPECT images over the tumor (*C*) and abdomen (C_B, σ_{BG}) at four hours after injection point.

Statistical analysis

We compare the four different sets of reconstruction correction parameter settings for ^{111}In-pentetreotide SPECT imaging. Tukey's test was used in GEP-NET patients (n = 20). Statistics were performed with IBM SPSS Statistics (version 23, IBM Corp., Armonk, NY). p <0.05 was considered significant.

RESULTS

Phantom study

The results of the SPECT QA phantom study were analyzed according to the EWW & OSEM from ^{111}In-pentetreotide SPECT. ^{111}In-pentetreotide SPECT image reconstruction conditions were compared using the parameter of CNR acquired from the SPECT QA phantom.

Figure 2 shows the optimum EWW from all typical window locations (set at about 171 keV and 245 keV) and four different sets of EWW parameters. When the hot rod diameter was 15, 20 or 30 mm, the CNR values using the energy window of 171 keV ± 10% and 245 keV ± 7.5% were significantly different than with the other parameters (p <0.05).

OSEM reconstruction conditions are plotted as the number of iterations in **Figure 3**. Determination of the iteration number using OSEM reconstruction conditions was also compared based on CNR. The number of Subsets was set at 8. The numbers of iterations were compared using different reconstruction parameters. The result showed that the highest CNR of OSEM reconstruction conditions was obtained with 8 subsets and 6 iterations (p <0.05).

Figure 4 shows the OSEM collection conditions obtained by CNR measured for ^{111}In-pentetreotide SPECT. This finding confirmed the LKS phantom study results. When NC, SC and AC were used, the CNR of the pancreas was significantly lower than that of liver (p <0.05). Representative axial phantom scan slices shown in **Figure 5** demonstrate the effects of SC, AC and CC on the tumor compartment and background.

Clinical study

Figure 6 shows the results of CNR of 20 GEP-NET patients evaluated by four different image correction methods obtained from ^{111}In-pentetreotide SPECT images. SC and AC did not result in a significantly different CNR from NC (p = 0.86). Only CC showed a significantly higher CNR, compared with NC and SC (p <0.05).

Figure 7 shows a representative case: a 66-year-old female with body mass index of 24.8 kg/m^2. A hypervascular pancreatic head lesion 15 mm in diameter was noted in early dynamic MRI, and post-surgical pathology confirmed it to be NET G2. Since the pancreatic head is located relatively deep in the

abdomen, ^{111}In-pentetreotide SPECT with NC showed weak visualization of the lesion. SPECT with CC showed better delineation of the lesion by the decreasing background noise and attenuation correction.

Discussion

Based on a phantom study, we determined EWW, OSEM reconstruction conditions (8 subsets and 6 iterations), and correction parameter settings for the CNR improvement of ^{111}In-pentetreotide SPECT images. In a clinical study of GEP-NETs cases, the CNR of the lesion when corrected with CC was significantly higher than with NC or SC.

The optimal EWW & OSEM reconstruction conditions improved the CNR for ^{111}In-pentetreotide SPECT acquisition**.** The ENETS consensus guidelines – the standard of care in NET – provide a tool to accurately assess the diagnosis of NETs, recommending that both photopeaks of ^{111}In are centered over 20% energy windows (*14*). In our study, we compared four different sets of EWW parameters based on this guideline. The optimal EWW was found to be 171 keV ± 10% and 245 keV ± 7.5%, compared with the guideline conditions. We thus recommend that

the optimal EWW should be set to 171 keV ± 10% and 245 keV ± 7.5% in clinic. In the OSEM algorithm, an excessive number of iterations might result in SPECT images that are too noisy (*15*).

Alexander HR, *et al*. reported that SRS missed one-third of all tumor lesions found by the surgery. SRS detected 30% of gastrinomas ≤1.1 cm, 64% of those 1.1 to 2 cm, and 96% of those >2 cm (*16*). To minimized false-negative diagnoses, Ruf J, *et al*. reported that AC in ^{111}In-pentetreotide SPECT/CT data has the potential to improve sensitivity, especially with a more centrally-localized focus (*17*). In our phantom study, CC in the pancreatic area showed a higher CNR than NC. This may have been due to attenuation and scatter corrections. Similar results were obtained in clinical studies (*18-20*).

Improvement of ^{111}In-pentetreotide SPECT diagnosis is needed for small tumors (<2 cm) (*21*). Although the reference image comparison, such as MRI, CT, is important in this case, careful observation of 111In-pentetreotide SPECT image is also necessary (*22-23*). Because SPECT/CT is not available at our hospital, we have used AC methods to automate the registration of CT medical images acquired from different modalities. This technique can be applied at any imaging

facility equipped with a SPECT scanner. We suggest that institutions without a SPECT/CT scanner should consider the optimal parameters for SPECT practice.

Our study had several limitations. Phantom study set the tumor and background radioactivity to 16:1. Radioactivity may not be support with all of clinical case. Optimum of EWW may not be enough to consider only two window widths of 20% and 15% of photo peak energy. A variety of EWWs should be compared. We have evaluated the optimal parameters for SPECT (E-CAM) practice. However, in other institutions, different SPECT devices may not exactly be compatible and support the same parameters. As a part of quality controls, each Center must check the optimal correction settings of their own SPECT device. The number of patients was small. Evaluation of a larger number of patients should be considered. Moreover, as the study was retrospective, differences in the types of NETs and distribution of the lesions could not be controlled. A greater variety of patients, based on grade, age and location of lesions, should be compared in the future study.

Conclusion

Attenuation and scatter correction of ^{111}In-pentetreotide SPECT can improve GEP-NETs imaging, with better contrast and the sharper lesion outlines than conventional SPECT imaging. In patients with GEP-NETs, optimal setting of SPECT parameters can improve the diagnostic accuracy of SPECT images, and therefore may lead to better-informed treatments.

Conflict of interest

The authors have no conflict of interests.

References

1) Yao JC, Hassan M, Phan A, et al. One hundred years after “carcinoid”: epidemiology of and prognostic factors for neuroendocrine tumors in 35,825 cases in the United States. *J Clin Oncol* 2008; 26: 3063–3072.

2) Ito T, Igarashi H, Jensen RT. Therapy of metastatic pancreaticneuroendocrine tumors (pNETs): recent insights and advances. *J Gastroenterol* 2012; 47: 941–60.

3) Ito T, Lee L, Hijioka M, et al. The up-to-date review of epidemiological pancreatic neuroendocrine tumors in Japan. *J Hepatobiliary* Pancreat Sci 2015; 22: 574–577.

4) Lloyd RV, Osamura RY, Klöppel G, Rosai J. WHO Classification of Tumours of Endocrine Organs. 4th Ed, Lyon: *IARC Press*; 2017.

5) Oberg K. State of the art and future prospects in the management of neuroendocrine tumors. *Q J Nucl Med* 2000; 44: 3–12.

6) Sharma P, Singh H, Bal C, Kumar R. PET/CT imaging of neuroendocrine tumors with (68)Gallium-labeled somatostatin analogues: an overview and single institutional experience from India. *Indian J Nucl Med* 2014; 29: 2–12.

7) Schillaci O, Spanu A, Scopinaro F, et al. Somatostatin receptor scintigraphy in liver metastasis detection from gastroenteropancreatic neuroendocrine tumors. *J Nucl Med* 2003; 44: 359–368.

8) Volterrani D, Orsini F, Chiacchio S. Multiagent targeting of neuroendocrine neoplasms. *Clin Transl Imaging* 2013; 1: 407–421.

9) Ito T, Sasano H, Tanaka M, et al. Epidemiological study of gastroenteropancreatic neuroendocrine tumors in Japan. *J Gastroenterol* 2010; 45(2): 234–243.

10) Hudson HM, Larkin RS. Accelerated Image Reconstruction Using Ordered Subsets of Projection Data. *IEEE Trans Med Imaging* 1994; 13: 601–609.

11) Ogawa K. Simulation study of triple-energy-window scatter correction in combined Tl-201, Tc-99m SPECT. *Ann Nucl Med* 1994; 8: 277–81.

12) Motomura N, Takahashi M, Nakagawara G, Iida H. Evaluation of a SPECT attenuation correction method using CT data registered with automatic registration software. 2003 IEEE Nuclear Science Symposium; Conference Record 2003; 4: 2676-2680.

13) Sreedhar K. Enhancement of Images Using Morphological Transformations. *Int*

J Comput Sci Inf Technol 2012; 4: 33–50.

14) Kwekkeboom DJ, Krenning EP, Scheidhauer K, et al. ENETS consensus guidelines for the standards of care in neuroendocrine tumors: Somatostatin receptor imaging with III In-pentetreotide. *Neuroendocrinology* 2009; 90(2): 184–189.

15) Gutman F, Gardin I, Delahaye N, et al. Optimisation of the OS-EM algorithm and comparison with FBP for image reconstruction on a dual-head camera: a phan- tom and clinical 18F-FDG study. *Eur J Nucl Med Mol Imaging* 2003; 30: 1510–1519.

16) Alexander HR, Fraker DL, Norton JA, et al. Prospective study of somatostatin receptor scintigraphy and its effect on operative outcome in patients with Zollinger-Ellison syndrome. *Ann Surg* 1998; 228(2): 228–238.

17) Ruf J, Steffen I, Mehl S, et al. Influence of attenuation correction by integrated low-dose CT on somatostatin receptor SPECT. *Nucl Med Commun* 2007; 28(10): 782–788

18) Ljungberg M, Strand SE. Attenuation and scatter correction in SPECT for sources in a nonhomogeneous object: A Monte Carlo study. *J Nucl Med* 1991;

32(6): 1278–1284.

19) Hutton BF, Buvat I, Beekman FJ. Review and current status of SPECT scatter correction. *Phys Med Biol* 2011; 56(14): 85–112

20) Rahmim A, Zaidi H. PET versus SPECT: strengths, limitations and challenges. *Nucl Med Commun* 2008; 29(3): 193-207

21) Fave GD, O'Toole D, Sundin A, et al. ENETS consensus guidelines update for gastroduodenal neuroendocrine neoplasms. *Neuroendocrinology* 2016; 103(2): 119–124

22) Reznek RH. CT/MRI of neuroendocrine tumours. *Cancer Imaging* : The Official Publication of the International Cancer Imaging Society 2006; 6: 163–177.

23) Dromain C, Déandréis D, Scoazec JY, et al. Imaging of neuroendocrine tumors of the pancreas. *Diagn Interv Imaging* 2016; 97(12): 1241–1257.

Fig.1

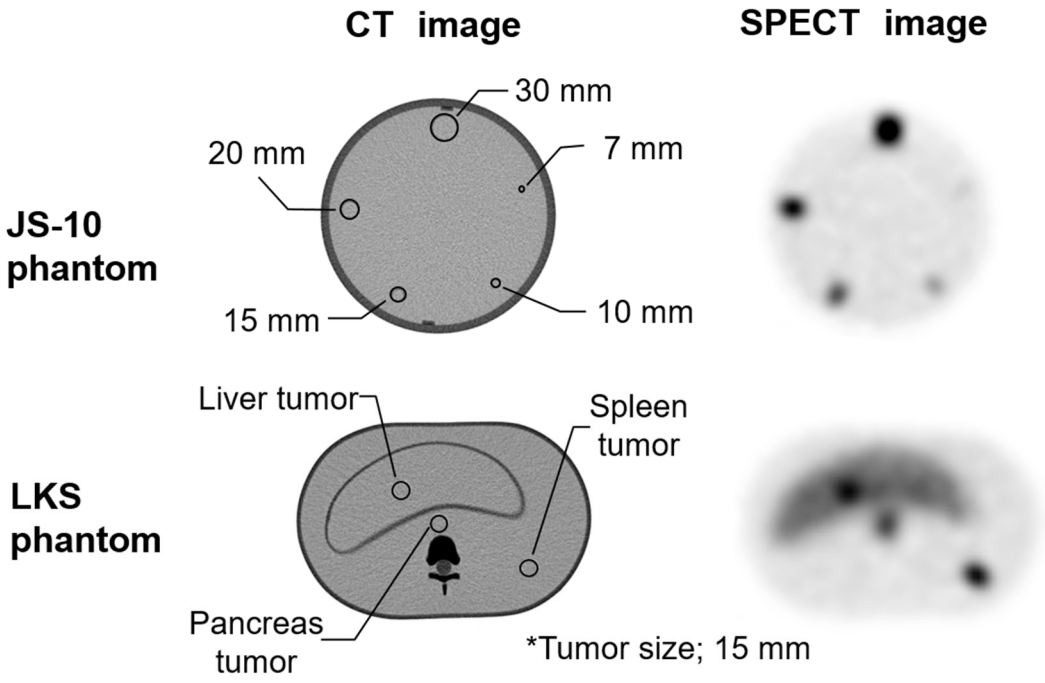

Fig. 1: Comparison of SPECT QA (JS-10) phantom images for energy window width, image reconstruction conditions and CT images, and anthropomorphic abdominal (LKS) phantom for image collection conditions.

Fig.2

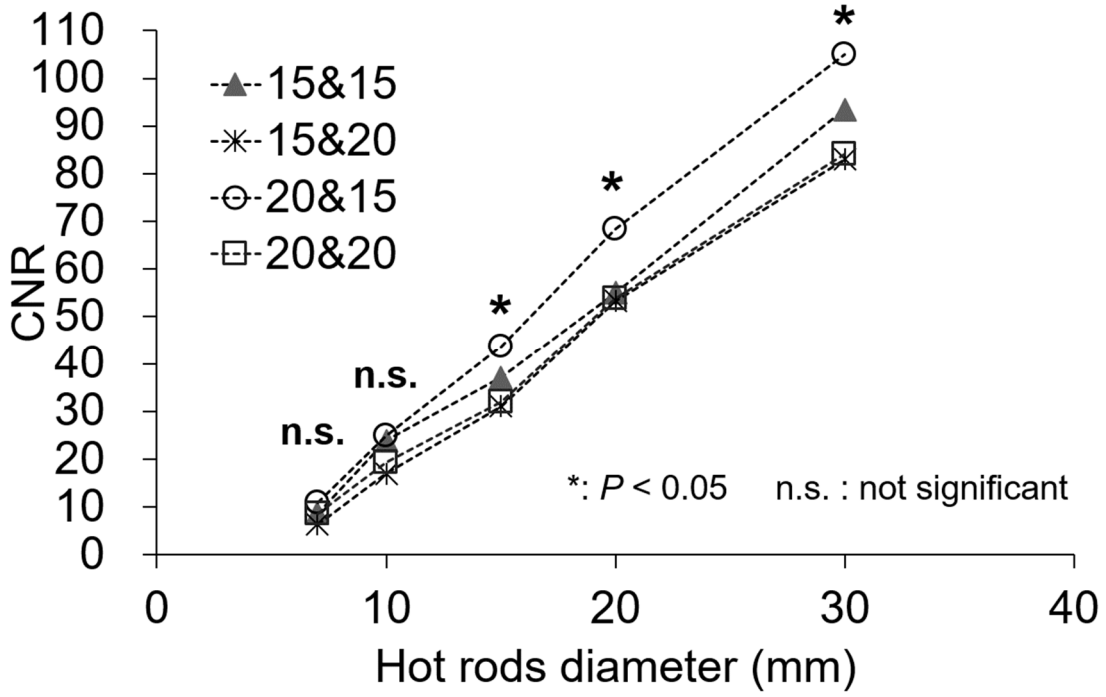

Fig. 2: CNR of hot rods for optimum EWW in the phantom study. The EWW setting of 171 keV ± 10% and 245 keV ± 7.5% was significantly better than other settings (p <0.05). * p <0.05, n.s., not significant.

Fig.3

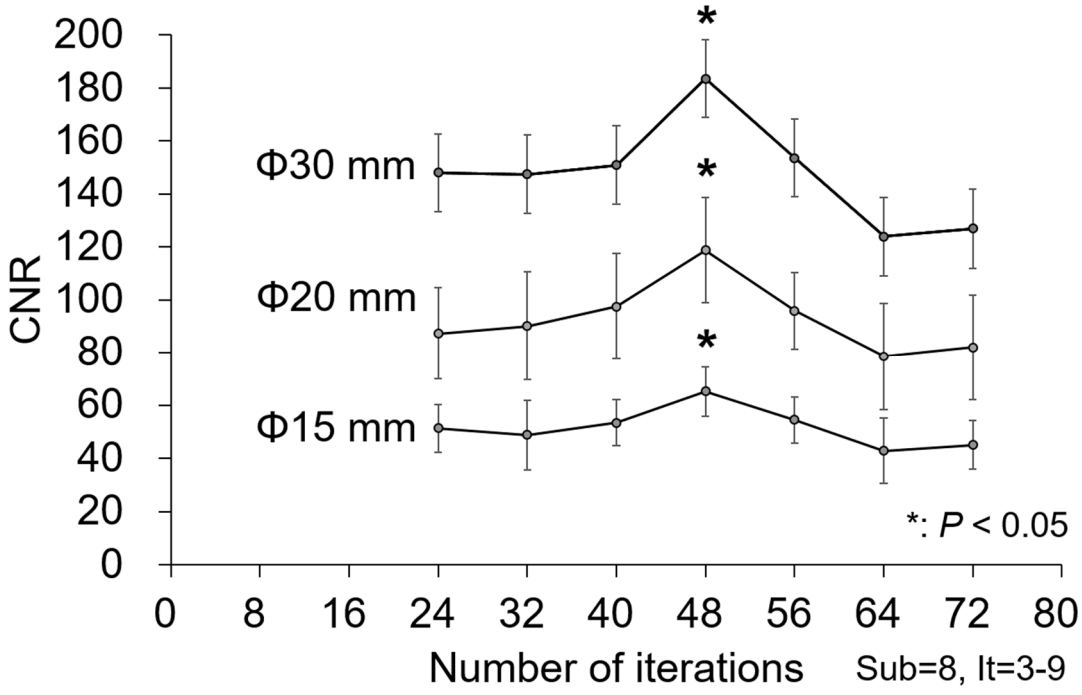

Fig. 3: Optimization of OSEM technique between CNR and numbers of iterations in the phantom study. OSEM reconstruction conditions of 8 subsets and 6 iterations gave significantly the highest CNR (p <0.05). * p <0.05, n.s., not significant.

Fig.4

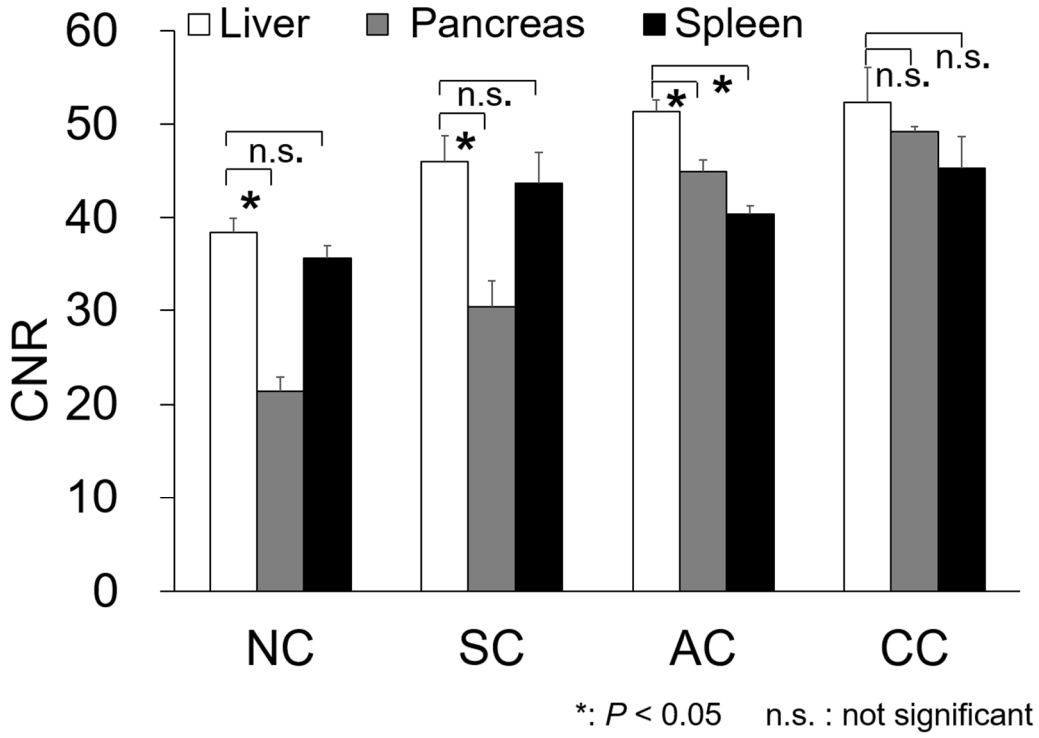

Fig. 4: Comparison of four techniques of SPECT image correction (NC, SC, AC, and CC) in the phantom study. Although underestimation occurred in the pancreas when NC and SC were used, CC showed no significant difference (p = 0.83). In particular, CC gave a significantly better CNR of the pancreas compared with NC, SC (p <0.05). * p <0.05, n.s., not significant.

Fig.5

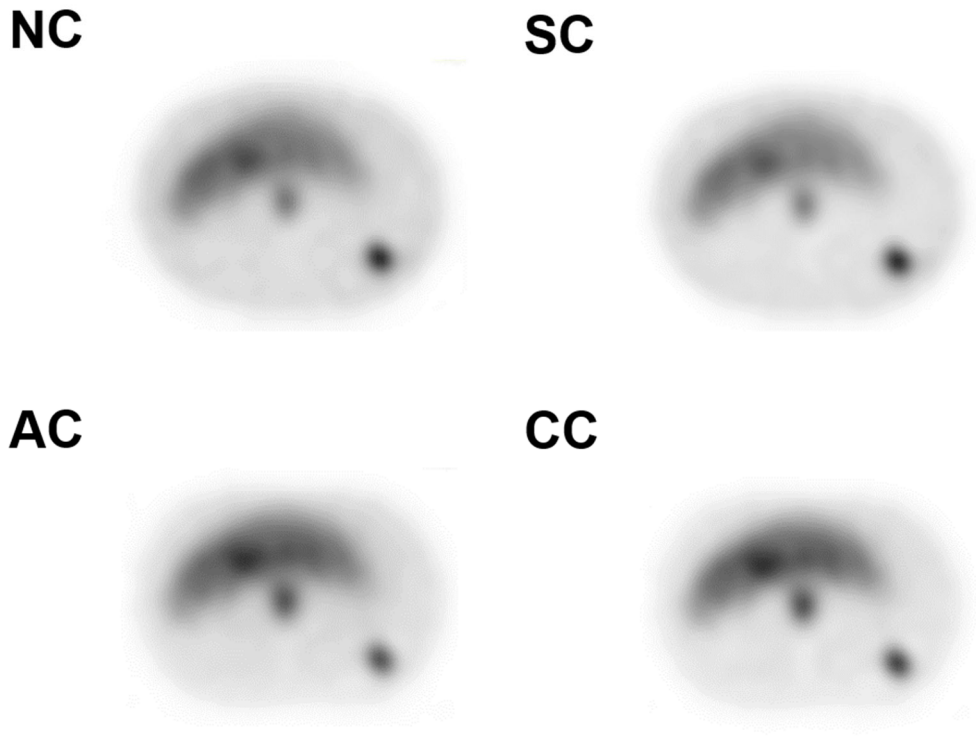

Fig. 5: Axial phantom SPECT images corrected by four methods (NC, SC, AC and CC) are shown.

Fig.6

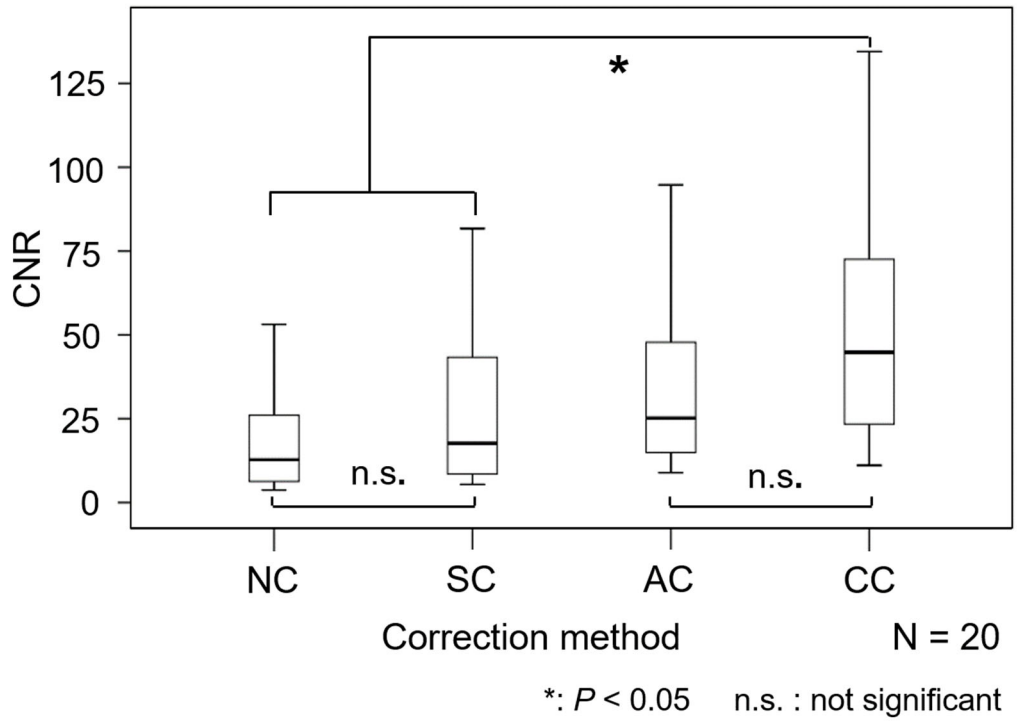

Fig. 6: Box plot of CNR evaluated by four methods (NC, SC, AC and CC) in 20 GEP-NET patients. NC and SC showed no significant difference (p = 0.86), while CC showed significant differences from NC and SC. * p <0.05, n.s., not significant.

Fig.7

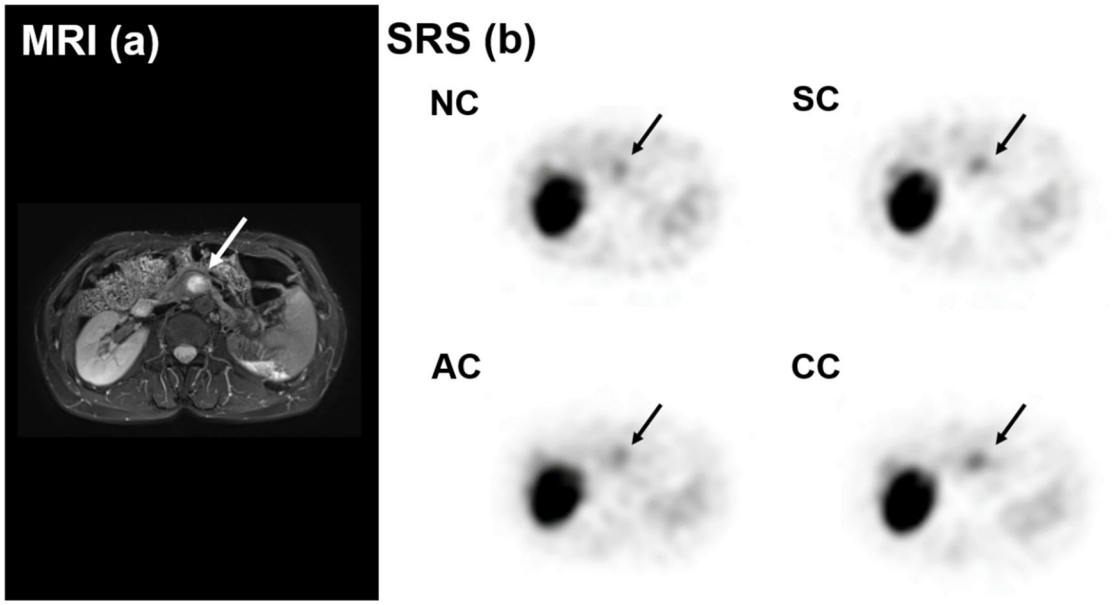

Fig. 7: Case with NET G1 of the pancreatic head without metastasis. (a) Highly-enhanced lesion in the pancreas is noted in early dynamic MRI image. (b) ^{111}In-pentetreotide SPECT images with NC, SC, AC and CC depicted abnormal uptake in the corresponding upper abdominal area (arrow). While images with SC and AC show comparable visualization of lesion with NC, CC shows the clearest delineation of the lesion.

Table 1

Characteristics	Patients (n = 20)
Age, mean ± SD (range), years	66.0 ± 15.6 (37-81)
Sex	
Men	13
Women	7
Final diagnosis	
Pancreatic NET	15
・*Stage*	
G1	7
G2	2
Unclear	6
Duodenal NET	2
Rectal NET	2
lymph node metastases of NET	1

NET, neuroendocrine tumor